Positional Isotope Exchange Analysis of the *Mycobacterium smegmatis* Cysteine Ligase (MshC)[†]

LaKenya Williams,[‡] Fan Fan,[§] John S. Blanchard,*[,§] and Frank M. Raushel*[,‡]

Department of Chemistry, P.O. Box 30012, Texas A&M University, College Station, Texas 77842-3012, and Department of Biochemistry, Albert Einstein College of Medicine, 1300 Morris Park Avenue, Bronx, New York 10461

Received February 26, 2008; Revised Manuscript Received March 7, 2008

ABSTRACT: MshC catalyzes the ATP-dependent condensation of GlcN-Ins and cysteine to form Cys-GlcN-Ins, which is an intermediate in the biosynthetic pathway of mycothiol, i.e., 1-D-*myo*-inosityl-2-(*N*-acetyl-L-cysteinyl)amido-2-deoxy-α-D-glucopyranoside (MSH or AcCys-GlcN-Ins). MSH is produced by *Mycobacterium tuberculosis*, members of the Actinomycetes family, to maintain an intracellular reducing environment and protect against oxidative and antibiotic induced stress. The biosynthesis of MSH is essential for cell growth, and therefore, the MSH biosynthetic enzymes present potential targets for inhibitor design. The formation of kinetically competent adenylated intermediates was suggested by the observation of positional isotope exchange (PIX) reaction using [$\beta\gamma$-$^{18}O_6$]-ATP in the presence of cysteine. The PIX rate depends on the presence of cysteine and increases with concentrations of cysteine. The loss of PIX activity upon the addition of small concentrations of pyrophosphatase suggests that the PP_i is free to dissociate from the active site of cysteine ligase into the bulk solution. The PIX activity is also eliminated at high concentrations of GlcN-Ins, consistent with the mechanism in which GlcN-Ins binds after cysteine−adenylate formation. This PIX analysis confirms that MshC catalyzes the formation of a kinetically competent cysteinyl-adenylate intermediate after the addition of ATP and cysteine.

INTRODUCTION

MshC catalyzes the ATP-dependent condensation of cysteine and 1-D-*myo*-inosityl-2-amido-2-deoxy-α-D-glucopyranoside (GlcN-Ins[1]) in the penultimate step of the biosynthetic pathway for mycothiol (MSH). MSH is the predominant low molecular weight thiol that protects actinomycetes against oxidative stress and cellular electrophilic toxins (*1–4*). MSH is synthesized via a series of enzymatic reactions (*5–8*) as illustrated in Scheme 1. The process is initiated by an *N*-acetyl-glucosamine transferase (MshA) to generate 3-phospho-GlcNAc-Ins, which is subsequently dephosphorylated to generate GlcNAc-Ins by an unknown phosphatase (*8*). GlcNAc-Ins is subsequently deacetylated by MshB, and the resulting GlcN-Ins is ligated with cysteine by MshC. The Cys-GlcN-Ins is then acetylated by MshD, yielding MSH. Mycobacteria generate the highest intracellular levels of MSH among actinomycetes (*9*). Studies have shown that *Mycobacterium smegmatis* mutants lacking MSH become more sensitive toward oxidizing agents, electrophiles, and antibiotics (*1–3*), suggesting a critical role of MSH in the survival and pathogenicity of mycobacteria (*1*).

We have chosen *Mycobacteria smegmatis* MshC for kinetic and mechanistic characterization. MshC from *M. smegmatis* has been recombinantly expressed, purified, and characterized (*10*). The enzyme is a monomer with a molecular weight of ∼47 kDa. The steady state kinetic mechanism of *M. smegmatis* MshC is Bi Uni Uni Bi ping−pong, with the ordered binding of ATP and L-cysteine, release of pyrophosphate, binding of GlcN-Ins, and finally the release of Cys-GlcN-Ins and AMP (*10*). On the basis of this kinetic mechanism, the overall reaction can be divided into two steps: cysteine adenylation and the subsequent ligation of cysteine to GlcN-Ins. Single-turnover reactions of the first and second half-reactions were determined using rapid-quench techniques, giving rates of ∼9.4 s^{-1} and ∼5.2 s^{-1}, respectively, consistent with the cysteinyl adenylate being a kinetically competent intermediate in the reaction by MshC (*10*). A stable bisubstrate analogue, 5′-*O*-[*N*-(L-cysteinyl)sulfamonyl]adenosine exhibits competitive inhibition versus ATP, noncompetitive inhibition versus cysteine, and an inhibition constant of ∼306 nM versus ATP.

Positional isotope exchange (PIX) has been used as a mechanistic probe for enzyme catalyzed reactions in which the individual atoms of a functional group within a substrate become torsionally equivalent in an intermediate or product during the reaction. PIX has been successfully used to determine the kinetic competence of reaction intermediates for a number of enzymes (*11, 12*) since it was first applied to the reaction catalyzed by glutamine synthetase by Midelfort and Rose (*13*).

[†] This work was supported in part by grants from the National Institute of Health (GM 33894 to F.M.R., AI33696 to J.S.B.), the Robert A. Welch Foudation (A-840 to F.M.R.), and a Fellowship from the Heiser Program for Research in Leprosy and Tuberculosis of The New York Community Trust to F.F.

* To whom correspondence should be addressed. Phone: (979) 845-3373; Fax: (979) 845-9452; E-mail: raushel@tamu.edu (F.M.R.). Phone: (718) 430-3096; Fax: (718) 430-8565; E-mail: blanchar@aecom.yu.edu (J.S.B.).

[‡] Texas A&M University.

[§] Albert Einstein College of Medicine.

[1] Abbreviations: PIX, positional isotope exchange; GlcN-Ins, 1-D-*myo*-inosityl-2-amido-2-deoxy-α-D-glucopyranoside; MSH, mycothiol.

10.1021/bi800327u CCC: $40.75
Published on Web 03/29/2008

Scheme 1

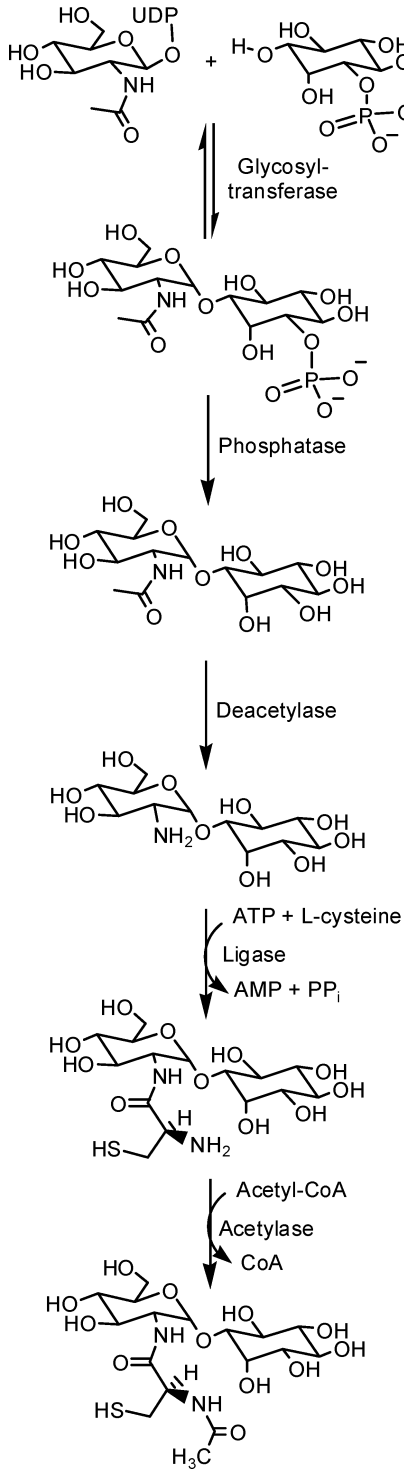

The two PIX reactions that could be catalyzed by MshC are outlined Scheme 2. When [$\beta\gamma$-$^{18}O_6$]-ATP is incubated with cysteine in the presence of MshC, pyrophosphate and cysteinyl-adenylate are expected to be formed (*10*). The ^{18}O-labels within the newly formed pyrophosphate can positionally scramble via two possible routes from this intermediate. If bond rotation is unrestricted for the original β-phosphoryl group of the newly formed pyrophosphate product, then ^{18}O will ultimately be found in the $\alpha\beta$-bridge position upon reversal of the first half-reaction and dissociation of ATP in the bulk solution. Alternatively, if the pyrophosphate formed within the active site can flip or dissociate and rebind to the enzyme, so as to interchange the positional identities of the original β- and γ-phosphoryl groups of ATP, then ^{16}O will be found in the γ-phosphoryl group of ATP. If rotation of the initially formed pyrophosphate product is torsionally and positionally unrestricted, then an equilibrium mixture of ATP will form with ^{18}O-labeling patterns represented by **I**, **II**, and **III**. However, if the pyrophosphate remains tightly bound such that only torsional equilibration of the β-phosphoryl group of ATP is allowed, then the formation of **III** is not possible. In this case, isotopic equilibration would be restricted to the equilibrium formation of **I** and **II**. Here, we report the results of positional isotope exchange experiments using *M. smegmatis* MshC to establish the participation of cysteinyl adenylate as a kinetically obligatory intermediate and to demonstrate that the pyrophosphate is free to dissociate and then reassociate with the cysteinyl adenylate enzyme complex.

MATERIAL AND METHODS

Oxygen-18 labeled potassium phosphate was prepared following the procedure of Risley and van Etten (*14*). Adenylate kinase (chicken muscle) and inorganic pyrophosphatase (*Escherichia coli*) were purchased from Sigma. $H_2{}^{18}O$ (90%) was purchased from Cambridge Isotope Laboratories. *Mycobacterium smegmatis* cysteine ligase (MshC) and 1-D-myo-inosityl-2-(*N*-acetyl-L-cysteinyl)amido-2-deoxy-α-D-glucopyranoside were prepared as previously described (*10*). All other materials were purchased from Sigma. Plasmid DNA for *Enterococcus faecalis* carbamate kinase was a generous gift from Dr. Vicente Rubio at Instituto de Investigaciones Citologicas in Valencia, Spain.

^{31}P Nuclear Magnetic Resonance Measurements. ^{31}P NMR spectra were acquired using a Varian Inova-400 NMR spectrometer operating at a frequency of 162 MHz. Acquisition parameters were 5000-Hz sweep width, 2.0 s acquisition time, and a 2.0 s delay between pulses.

Preparation of [$\beta\gamma$ -$^{18}O_6$]-ATP. The labeled ATP was synthesized from ^{18}O-labeled carbamoyl phosphate, AMP, a trace of ATP, adenylate kinase, and carbamate kinase as outlined by Cohn and Hu with slight modifications (*15*). Labeled carbamoyl phosphate was synthesized chemically by adding 1.25 mL of 6 M KCNO to a 1.0 mL sodium acetate solution, pH 4.8, containing 400 mg of Na_2P_i (^{18}O). The solution was incubated at room temperature while continuously monitoring and adjusting the pH to ~6.5 with 10% acetic acid. After 20 min, 600 μL of 6 M KCNO was added and the mixture incubated for an additional 15 min. After the formation of carbamoyl phosphate was confirmed by ^{31}P NMR, the solution was chilled and then added in aliquots to the ATP reaction mixture. The ATP reaction mixture contained 1250 μmol of AMP, 20 μmol of ATP, 2550 μmol of $MgCl_2$, 1.5 mmol of KCl, 400 mM Tris-HCl at pH 7.6, 500 units of adenylate kinase, and 1000 units of carbamate kinase. After the addition of all components, the reaction mixture contained 40 mM AMP, 0.6 mM ATP, 50 mM $MgCl_2$, 0.4 M Tris-HCl at pH 7.3, and 0.2 M KCl. After all of the carbamoyl phosphate had been added, the mixture was incubated at 35 °C for 30 min. The production of ATP was confirmed by ^{31}P NMR spectroscopy, and the reaction was terminated by the addition of 2 drops of CCl_4. The reaction mixture was applied to a

Scheme 2

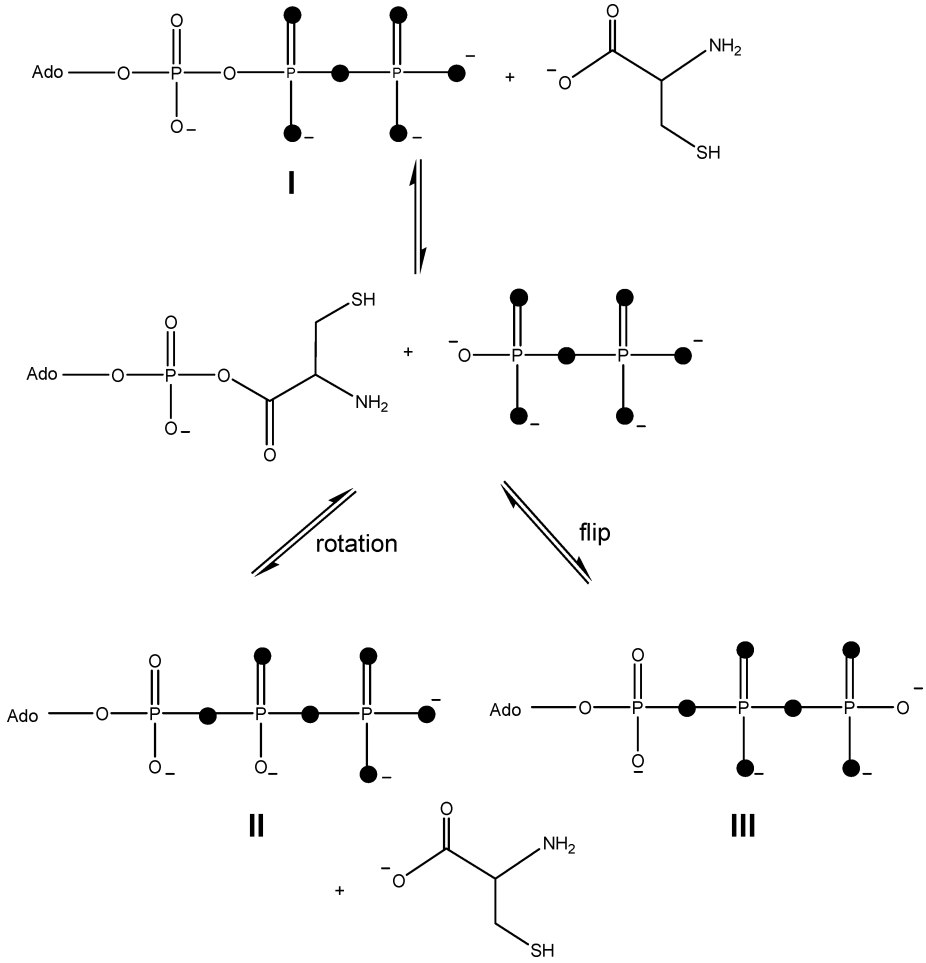

DEAE-Sephadex column and eluted with a 2 L gradient (0–1.0 M) of TEA-CO_2 (TEA; triethylamine) buffer at pH 7.6. All fractions containing ATP were pooled and concentrated in a rotary evaporator to near dryness and washed with 3 volumes of methanol, dissolved in water, and then titrated to pH 9 with KOH. Analysis of ^{18}O content was achieved by ^{31}P NMR spectrsocopy. Shown in Figure 1 are the α and γ resonances of [$\beta\gamma$-$^{18}O_6$]-ATP. The ^{18}O content of the ATP at the indicated positions was 89%.

Positional Isotope Exchange Reaction. The positional isotope exchange was monitored as a function of time by following the incorporation of ^{18}O from [$\beta\gamma$-$^{18}O_6$]-ATP into the α-β bridge position. The reaction mixtures contained 5.0 mM [$\beta\gamma$-$^{18}O_6$]-ATP, 5.0 mM $MgCl_2$, 2.0 mM DTT, 1.0 mM L-cysteine, 100 mM HEPES at pH 7.8, and 5 μM cysteine ligase. The total volume of the assay was brought to 5.25 mL and incubated at 35 °C for 5 h. A 500 μL aliquot was removed every hour and each aliquot quenched by adding 125 μL of 1.0 M EDTA and 125 μL of D_2O. The samples were centrifuged to remove any precipitated protein and the solution transferred to an NMR tube. Experiments with the inclusion of pyrophosphatase contained this enzyme at concentrations ranging from 0.001–0.05 units. The total volume of each assay was 500 μL, and the reactions were quenched and treated as previously described.

Positional Isotope Exchange as a Function of L-Cysteine Concentration. Reactions with variable concentrations of L-cysteine contained 5.0 mM [$\beta\gamma$-$^{18}O_6$]-ATP, 5.0 mM $MgCl_2$, 2.0 mM DTT, 100 mM HEPES at pH 7.8, 5 μM cysteine ligase, and L-cysteine ranging from 0.05–20 mM. The assay volume was 500 μL, and the samples were incubated at 35 °C for 2 h and quenched by adding 125 μL of 1.0 M EDTA and 125 μL of D_2O.

Positional Isotope Exchange Inhibition by GlcN-Ins. Reactions with variable concentrations of GlcN-Ins contained 5.0 mM [$\beta\gamma$-$^{18}O_6$]-ATP, 5.0 mM $MgCl_2$, 2.0 mM DTT, 6.0 mM L-cysteine, 100 mM HEPES at pH 7.8, 5 μM cysteine ligase, and GlcN-Ins ranging from 0.1–2.5 mM. The volume of the assays was 500 μL, and the samples were incubated at 35 °C for 2 h and quenched as previously outlined.

RESULTS

Positional Isotope Exchange. The formation of a cysteine−adenylate intermediate in the cysteine ligase catalyzed reaction was addressed by measurement of a PIX reaction within [$\beta\gamma$-$^{18}O_6$]-ATP (**I**). When [$\beta\gamma$-$^{18}O_6$]-ATP was incubated with MshC in the absence of L-cysteine, there was no detectable scrambling of the ^{18}O labels within ATP (data not shown). However, positional scrambling of the ^{18}O-labels within ATP was observed upon incubation of cysteine ligase, [$\beta\gamma$-$^{18}O_6$]-ATP, and L-cysteine (Figure 2A−C). Incorporation of an ^{18}O into the α-β bridge position of ATP results in the appearance of a new ^{31}P NMR resonance for the α-P that is 0.017 ppm upfield from the ^{16}O resonance (*15*). There is a decrease in the percentage of the ^{16}O species in the starting

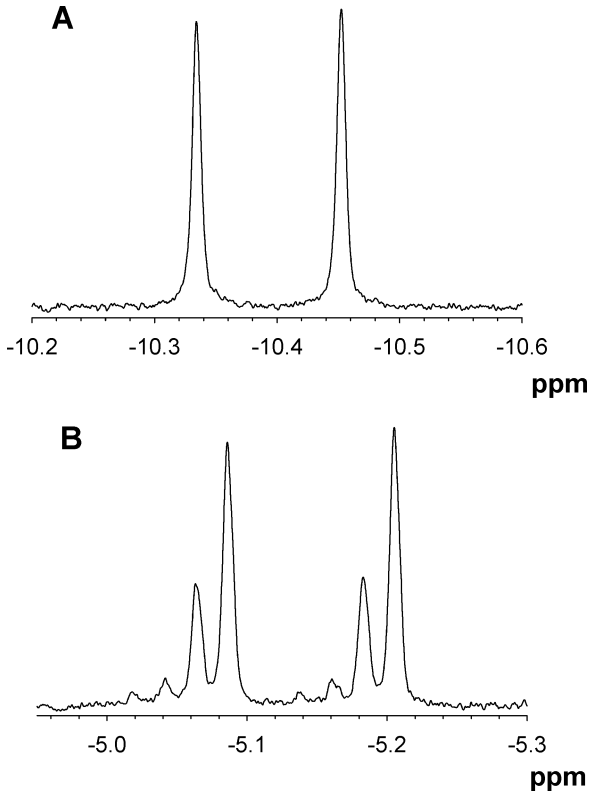

FIGURE 1: ^{31}P NMR spectra of the [$\beta\gamma$ -$^{18}O_6$]-ATP (I) substrate used in this investigation. (A) ^{31}P NMR resonance of the α-P and (B) ^{31}P NMR resonance of the γ-P. Additional details are provided in the text.

material from 100% to 76%, 58%, and 46% after 60, 90, and 120 min, respectively, as illustrated in Figure 2A−C. There is also a corresponding increase in the fraction of the ^{31}P NMR resonance for the species that contains an ^{18}O-label in the α-β bridge position. The time dependence for the fraction of each species is plotted in Figure 2D. An ^{18}O label will be found in the α-β bridge position of ATP only if the P−O bond to the α-P is broken and the newly formed β-phosphoryl group allowed free rotation within in the active site. Alternatively, the newly formed PP_i could rotationally interchange β- and γ-phosphoryl groups to γ- and β-phosphoryl groups. In either case, an ^{18}O will appear in the α-β bridge position of ATP (**II** or **III**). However, an ^{16}O atom will migrate to the γ-P only if the newly formed PP_i is allowed to completely flip within the active site and the positional identities of the β- and γ-phosphoryl groups are interchanged (as observed in structure **III**).

These results demonstrate that the adenylation of cysteine is reversible, but they provide no information about the torsional or positional equilibrium that pyrophosphate can undergo within the active site of MshC. The PIX reaction resulting from the positional randomization of PP_i was monitored by measuring the fractional decrease of the [γ-$^{18}O_4$]-P species of the labeled ATP as a function of time. Initially, the [γ-$^{18}O_4$]-P species represents 63% of the total NMR signal at time zero for the γ-P because each of the 4 oxygens bonded to this phosphorus are 89% ^{18}O. After the addition of enzyme for 60, 90, and 120 min, the percentage of this species decreases to 53%, 45%, and 39% of the total NMR signal for the γ-resonance (Figure 3A−C). The isotopic composition changes at the γ-P as a function of time are shown in Figure 3D.

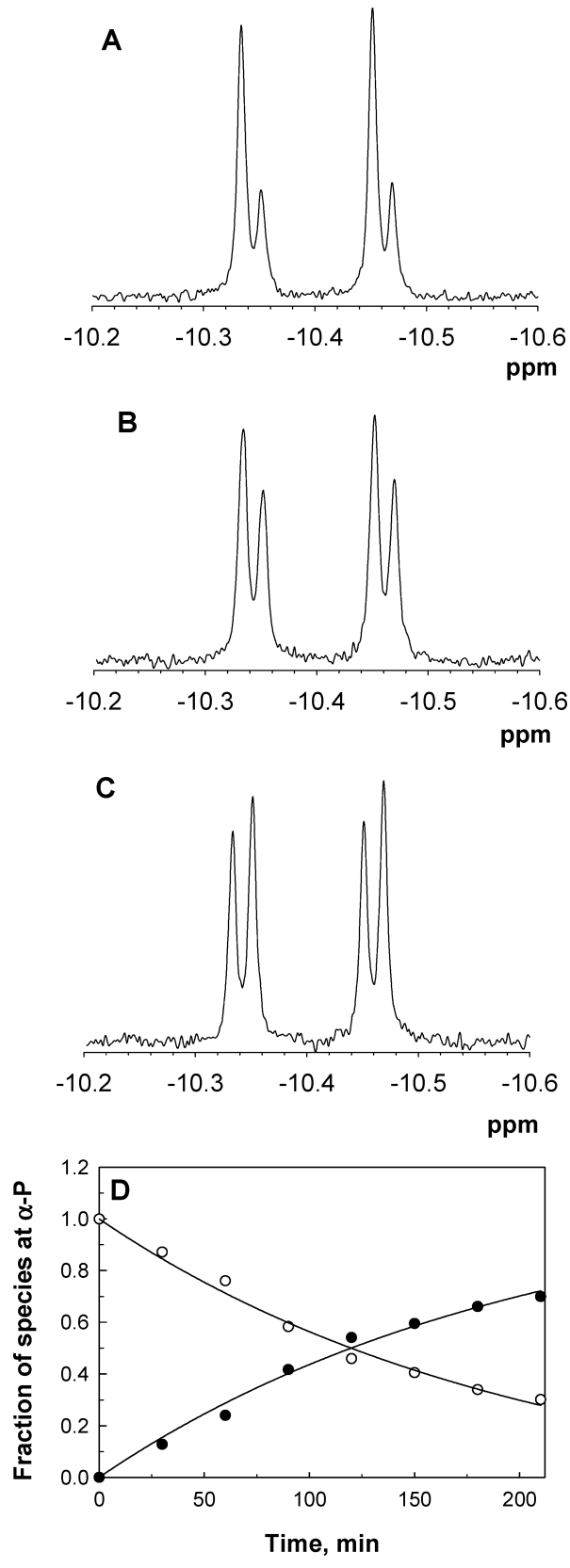

FIGURE 2: ^{31}P NMR spectra for changes in the isotopic composition of the α-P of ATP as a function of time (A) 60 min; (B) 90 min; (C) 120 min; and (D) the fractional occurrence of ^{16}O (○) and ^{18}O (●) in the αβ-bridge position of ATP as a function of time. Additional details are provided in the text.

The rate constant for the progression of positional isotopic equilibrium within the α-P was obtained by fitting of the data in Figure 2D to eq 1. This equation takes into account

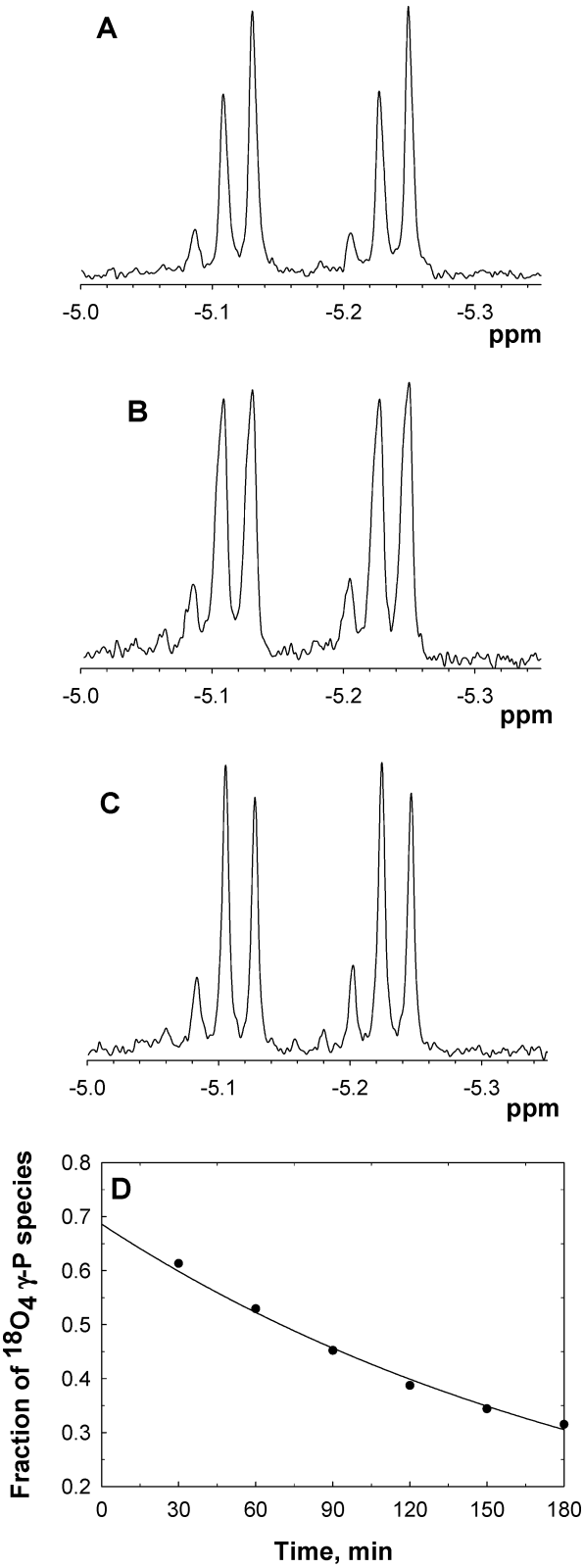

FIGURE 3: ^{31}P NMR spectra for changes in the isotopic compositon of the γ-P species of ATP as a function of time. (A) 60 min; (B) 90 min; (C) 120 min; and (D) the fractional occurrence of the $^{18}O_4$-γ-P species as a function of time. Additional details are provided in the text.

the fraction of ^{18}O labeling and the number of species possible for the PIX reaction. In this equation, X_o is the amount of the [α-$^{16}O_4$]-P species at time t, X_t is the total NMR signal for all possible α-P species, z is the fraction of ^{18}O labeling (0.89), n is the number of species that display

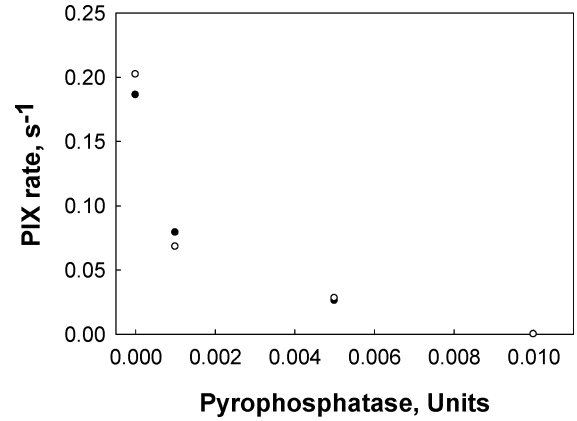

FIGURE 4: PIX rates at the α-P (●) and γ-P (○) of ATP as a function of the amount of pyrophosphatase added to the assay. Additional details are provided in the text.

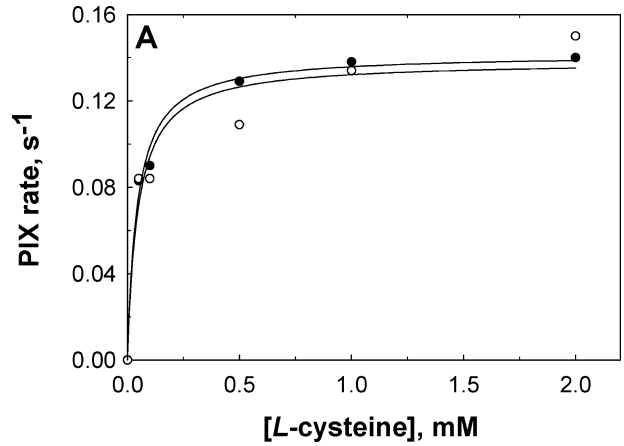

FIGURE 5: PIX rate as a function of the concentration of cysteine. The PIX rates as measured from the exchange at the α-P (●) and γ-P (○) of ATP. Additional details are provided in the text.

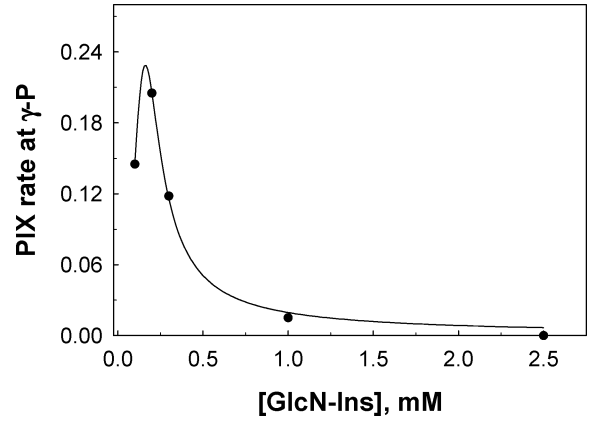

FIGURE 6: Change in the rate of the PIX reaction as a function of the concentration of GlcN-Ins.

^{18}O exchange for a particular PIX reaction, and m is the number of species that do not display exchange. For the two mechanisms outlined in Scheme 2, if the β-phosphoryl group is only allowed to torsionally equilibrate via *rotation*, then $n = 2$ and $m = 1$. If, however, the PP_i is allowed to *flip*, then $n = 5$ and $m = 1$ since the positional identities of the β- and γ-phosphoryl groups will be lost. The data were fitted to both models, but the results were only compatible with a fit to eq 1 for the model where $n = 5$ and $m = 1$. The rate constant for the positional isotopic equilibration of the α-P

Scheme 3

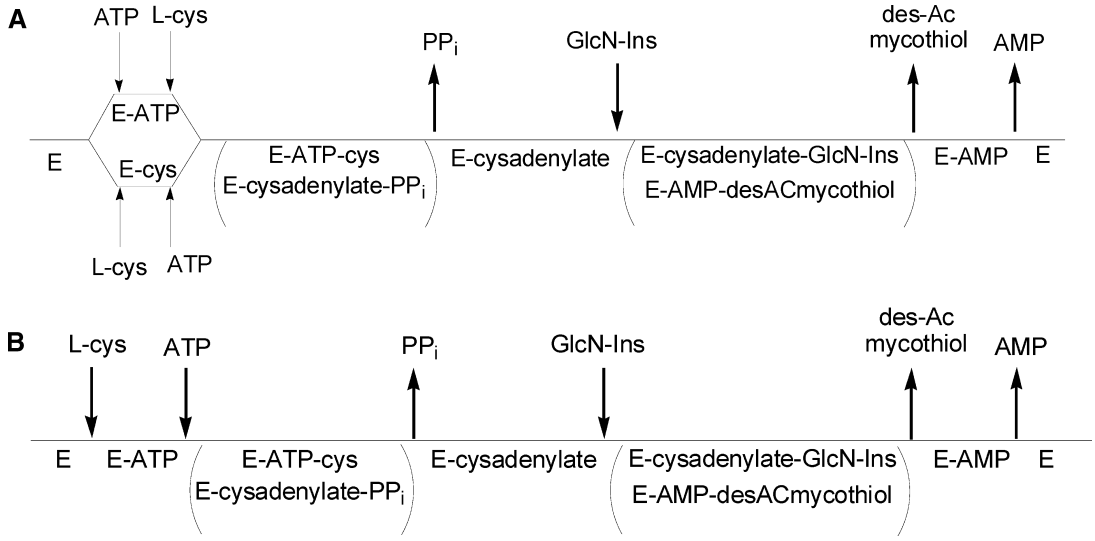

is 0.005 ± 0.001 min^{-1}, and the corresponding turnover number for the PIX reaction under these conditions was calculated to be 5 ± 1 min^{-1} ((0.005 min^{-1})(5000 μM ATP/5 μM enzyme)).

The rate constant for the equilibration of the γ-P was obtained in a similar manner. The PIX reaction that alters the isotopic composition of the γ-P can occur only by the flipping of PP_i. The number of species (n) that will show a reduction in the fraction of [γ-$^{18}O_4$]-P is 3, and the number of species (m) that will not result in a decrease in the fraction of [γ-$^{18}O_4$]-P is 3. In eq 2, Y_4 is the amount of the [γ-$^{18}O_4$]-P species at time t, Y_t is the sum of all isotopic species at the γ-P, and all other values are as previously defined. Fitting the experimental data presented in Figure 3D for the γ-P to eq 2 yields a rate constant for the approach to equilibrium of 0.005 ± 0.002 min^{-1}. The turnover number for the PIX reaction at the γ-P is 5 ± 2 min^{-1}.

$$\frac{X_o}{X_t} = 1 + \frac{zne^{-kt}}{n+m} - \frac{zn}{n+m} \quad (1)$$

$$\frac{Y_4}{Y_t} = z^4\left(1 + \frac{ne^{-kt}}{n+m} - \frac{n}{n+m}\right) \quad (2)$$

These results are only consistent with a complete torsional and positional reorientation of the PP_i upon formation of the cysteine−adenylate intermediate. However, these results do not distinguish between the complete reorientation within the active site or an alternative mechanism where the PP_i product dissociates from the active site and then randomly rebinds to the active site of the enzyme. If the PP_i dissociates from the active site of cysteine ligase into the bulk solution, the PIX reaction should be suppressed if the assays are conducted in the presence of inorganic pyrophosphatase. The pyrophosphatase will effectively prevent the PP_i product from reentering the active site through the irreversible hydrolytic cleavage to inorganic phosphate. Alternatively if the complete reorientation of PP_i occurs within the active site without dissociation, then pyrophosphatase would have no effect on the observed rate of the PIX reaction. A PIX reaction was observed at very low concentrations of pyrophosphatase but increasing the concentration of pyrophosphatase to as little as 0.01 units per assay diminished the PIX activity to undetectable levels. Therefore, the pyrophosphate product is able to completely dissociate from the active site of cysteine ligase and reenter the active site with complete randomization of the original β- and γ-phosphoryl substituents. The effect of increasing pyrophosphatase on the PIX rate is shown in Figure 4.

Positional Isotope Exchange Enhancement by L*-Cysteine.* In the analysis of the substrate binding order for the first sequential segment of the reaction catalyzed by cysteine ligase, the concentration of L-cysteine was varied at a fixed concentration of ATP and in the absence of GlcN-Ins. The rate of the PIX reaction increased hyperbolically when ATP and enzyme are incubated at concentrations of L-cysteine up to 4 mM. The PIX rates were plotted as a function of L-cysteine concentration, and the data are shown in Figure 5.

The data were fitted to eq 3 to obtain the rate constant for the PIX reaction at saturating concentration of L-cysteine. The rate constant for the PIX reaction at the α-P is 8.5 ± 0.3 min^{-1}, and the rate constant for the PIX reaction at the γ-P is 8.3 ± 0.6 min^{-1}.

$$v/E_t = (V_{ex}A)/(K_m + A) \quad (3)$$

Positional Isotope Exchange Inhibition by GlcN-Ins. In the second step of the proposed cysteine ligase reaction, GlcN-Ins attacks the cysteine−adenylate intermediate to form the product Cys-GlcN-Ins. To analyze the binding order of this reaction, L-cysteine and ATP were incubated with varying concentrations of GlcN-Ins. There is a modest increase in the rate of PIX up to 0.2 mM GlcN-Ins; however, there is a dramatic decrease in rate as the concentration of GlcN-Ins is increased to 0.3 mM. Increasing the concentration of GlcN-Ins to 2.5 mM abolished all of the PIX activity. The rate constants for the PIX reactions at the γ-P were calculated using eq 2, and the data for the variation of GlcN-Ins are presented in Figure 6. These data were fit to eq 4, where B represents the concentration of GlcN-Ins, K_b is the enhancement constant, and K_i is the inhibition constant for the effect induced by the varied substrate (*16*). The values obtained from the fit were 0.26 ± 0.01 and 0.10 ± 0.01 mM for the K_i and K_b, respectively.

$$v = \frac{VB}{K_b + B + \frac{B^2}{K_i}} \quad (4)$$

DISCUSSION

Positional isotope exchange has been used to verify the existence of enzyme-bound intermediates in the pantothenate synthetase (*17*), GMP synthetase (*18*), and carbamoyl phosphate synthetase reactions (*19*). The reactions of GMP synthetase, pantothenate synthetase, and cysteine ligase are similar, and these enzymes utilized ATP to activate the cosubstrate for nucleophilic attack through the formation of adenylated intermediates. The PIX technique has been used to confirm the formation of these intermediates and to provide insight about the substrate binding order.

The positional isotope exchange of [$\beta\gamma$-$^{18}O_6$]-ATP (**I**) to ATP (**II** or **III**) as catalyzed by MshC is observed only in the presence of L-cysteine. Incubation of ATP (**I**) with cysteine ligase in the absence of L-cysteine showed no positional isotope exchange. This result is consistent with the direct attack of the carboxyl group of L-cysteine on the α-phosphate of ATP (**I**) and the reformation of ATP (**II** or **III**) by the attack of PP_i on the cysteine−adenylate intermediate. The formation of ATP (**III**) with an interchange of the β- and γ-phosphoryl groups supports a mechanism that requires the complete reorientation of PP_i prior to reformation of ATP. The observed rate constants for positional isotope exchange involving the α-P and γ-P are experimentally the same, suggesting that the flipping of PP_i is unrestricted relative to the rotation at the β-phosphoryl group. The dissociation/reassociation of PP_i was assessed by the inclusion of inorganic pyrophosphatase in the PIX assay. The loss of PIX activity upon the addition of low concentrations of pyrophosphatase establishes that PP_i is free to dissociate from, and rebind to, the active site of cysteine ligase. Once PP_i dissociates from the active site, the positional identities of the β- and γ-phosphoryl groups are lost. PP_i reenters the active site, attacks the cysteine−adenylate intermediate, and scrambles the isotopic labels within the newly formed ATP (**I**, **II**, and **III**).

The substrate binding order of cysteine ligase was investigated by using the PIX methodology. In an analysis of the first chemical event, the concentration of L-cysteine was varied with ATP (**I**) at a fixed concentration, and the rate of the PIX reactions was measured. The rate of the PIX reaction increased to a maximum as the concentration of L-cysteine exceeds 0.5 mM. The ordered binding of ATP and cysteine has been suggested previously (*10*); however, if ATP binds first to the enzyme, increasing the concentration of cysteine would inhibit the PIX rate since saturating levels of cysteine will prevent ATP from dissociating from the enzyme. However, if cysteine must bind prior to ATP, then increasing levels of cysteine will have no effect on the dissociation rate of ATP from the enzyme. In this case, the PIX rate would increase as the enzyme−cysteine binary complex becomes saturated. A random kinetic mechanism for the binding of substrates to the active site would be indistinguishable from a kinetic mechanism that required the binding of cysteine prior to the binding of ATP. In the PIX experiments reported here, the rate of the PIX reactions increased with the concentration of L-cysteine, but no inhibition was detected at substrate concentrations up to 100 times the K_m value. This result thus supports a kinetic mechanism for MshC that is either random (as in Scheme 3A) or one in which L-cysteine binds prior to ATP (Scheme 3B).

Addition of GlcN-Ins to the PIX assays was used to probe the second step of the cysteine ligase reaction. The second step involves the release of PP_i, binding of GlcN-Ins, and the reaction of the third substrate with the cysteine−adenylate intermediate to form the ultimate products Cys-GlcN-Ins and AMP. The observed PIX activity was abolished at high concentrations of GlcN-Ins. In a Bi Uni Uni Bi ping−pong kinetic mechanism, this result demonstrates that the dissociation of pyrophosphate from the active site is faster than the reformation of ATP and cysteine from the enzyme-bound PP_i and the cysteine−adenylate intermediate. However, if the release of PP_i is not required for the binding of the third substrate, GlcN-Ins, then this result demonstrates that the reaction of GlcN-Ins with the intermediate is faster than the net rate constant for the regeneration and dissociation of ATP from the active site.

As an extension of our previous mechanistic characterization of MshC (*10*), PIX experiments using [$\beta\gamma$-$^{18}O_6$]-ATP were performed to validate the steady state kinetic mechanism for the MshC-catalyzed condensation reaction of cysteine to GlcN-Ins. A PIX reaction with ^{18}O-labeled ATP was only observed in the presence of cysteine. The rate of the PIX reaction increased at high concentrations of cysteine, but no inhibition of this activity was observed at concentrations up to 100-fold greater than the Michaelis constant for cysteine. This result is consistent with either a random mechanism or one in which cysteine must bind before ATP. The loss of PIX activity upon the addition of pyrophosphatase suggests that PP_i is free to dissociate from the active site of cysteine ligase into the bulk solution. The PIX activity is also eliminated at high concentrations of GlcN-Ins, consistent with the mechanism in which GlcN-Ins binds after the formation of the cysteine−adenylate intermediate. This PIX analysis confirms that MshC catalyzes the formation of a kinetically competent cysteinyl−adenylate intermediate after the addition of ATP and cysteine.

REFERENCES

1. Newton, G. L., Av-Gay, Y., and Fahey, R. C. (2000) A novel mycothiol-dependent detoxification pathway in mycobacteria involving mycothiol *S*-conjugate amidase. *Biochemistry 39*, 10739–10746.
2. Newton, G. L., Unson, M. D., Anderberg, S. J., Aguilera, J. A., Oh, N. N., delCardayre, S. B., Av-Gay, Y., and Fahey, R. C. (1999) Characterization of *Mycobacterium smegmatis* mutants defective in 1-d-myo-inosityl-2-amino-2-deoxy-alpha-d-glucopyranoside and mycothiol biosynthesis. *Biochem. Biophys. Res. Commun. 255*, 239–244.
3. Rawat, M., Newton, G. L., Ko, M., Martinez, G. J., Fahey, R. C., and Av-Gay, Y. (2002) Mycothiol-deficient *Mycobacterium smegmatis* mutants are hypersensitive to alkylating agents, free radicals, and antibiotics. *Antimicrob. Agents Chemother. 46*, 3348–3355.
4. Buchmeier, N. A., Newton, G. L., Koledin, T., and Fahey, R. C. (2003) Association of mycothiol with protection of *Mycobacterium tuberculosis* from toxic oxidants and antibiotics. *Mol. Microbiol. 47*, 1723–1732.
5. Anderberg, S. J., Newton, G. L., and Fahey, R. C. (1998) Mycothiol biosynthesis and metabolism. Cellular levels of potential intermediates in the biosynthesis and degradation of mycothiol in *Mycobacterium smegmatis*. *J. Biol. Chem. 273*, 30391–30397.

6. Bornemann, C., Jardine, M. A., Spies, H. S., and Steenkamp, D. J. (1997) Biosynthesis of mycothiol: elucidation of the sequence of steps in *Mycobacterium smegmatis*. *Biochem. J. 325*, 623–629.
7. Newton, G. L., and Fahey, R. C. (2002) Mycothiol biochemistry. *Arch. Microbiol. 178*, 388–394.
8. Newton, G. L., Ta, P., Bzymek, K. P., and Fahey, R. C. (2006) Biochemistry of the initial steps of mycothiol biosynthesis. *J. Biol. Chem. 281*, 33910–33920.
9. Newton, G. L., Arnold, K., Price, M. S., Sherrill, C., Delcardayre, S. B., Aharonowitz, Y., Cohen, G., Davies, J., Fahey, R. C., and Davis, C. (1996) Distribution of thiols in microorganisms: mycothiol is a major thiol in most actinomycetes. *J. Bacteriol. 178*, 1990–1995.
10. Fan, F., Luxenburger, A., Painter, G. F., and Blanchard, J. S. (2007) Steady-state and pre-steady-state kinetic analysis of *Mycobacterium smegmatis* cysteine ligase (MshC). *Biochemistry 46*, 11421–11429.
11. Mullins, L. S., and Raushel, F. M. (1995) Positional isotope exchange as probe of enzyme action. *Methods Enzymol. 249*, 398–425.
12. Raushel, F. M., and Villafranca, J. J. (1988) Positional isotope exchange. *CRC Crit. Rev. Biochem. 23*, 1–26.
13. Midelfort, C. F., and Rose, I. A. (1976) A stereochemical method for detection of ATP terminal phosphate transfer in enzymatic reactions. Glutamine synthetase. *J. Biol. Chem. 251*, 5881–5887.
14. Risley, J. M., and Van Etten, R. L. (1978) A convenient synthesis of crystalline potassium phosphate - $^{18}O_4$ (monobasic) of high isotopic purity. *J. Labelled Compd. Radiopharm. 15*, 544–548.
15. Cohn, M., and Hu, A. (1980) Isotopic oxygen-18 shifts in phosphorus-31 NMR of adenine nucleotides synthesized with oxygen-18 various position. *J. Am. Chem. Soc. 102*, 913–916.
16. Cleland, W. W. (1967) *Adv. Enzymol. Relat. Areas Mol. Biol.*, pp 1–32.
17. Williams, L., Zheng, R., Blanchard, J. S., and Raushel, F. M. (2003) Positional isotope exchange analysis of the pantothenate synthetase reaction. *Biochemistry 42*, 5108–5113.
18. von der Saal, W., Crysler, C. S., and Villafranca, J. J. (1985) Positional isotope exchange and kinetic experiments with *Escherichia coli* guanosine-5′-monophosphate synthetase. *Biochemistry 24*, 5343–5350.
19. Raushel, F. M., and Villafranca, J. J. (1980) Phosphorus-31 nuclear magnetic resonance application to positional isotope exchange reactions catalyzed by *Escherichia coli* carbamoyl-phosphate synthetase: analysis of forward and reverse enzymatic reactions. *Biochemistry 19*, 3170–3174.

BI800327U